Aspects on the Numerical Modelling of Rock Mass Anisotropy in Tunnelling

By Roland Leitner, Markus Pötsch and Wulf Schubert

The orientation of discontinuities relative to an underground structure has a big influence on the response of the rock mass to excavation (1). Stress redistribution and displacements depend on the direction-dependent properties of the rock mass, usually referred to as anisotropy. Anisotropy can be a result of phyllosilicates, especially in metamorphic rock types, and its arrangement in layers. Brittle faulting can create or intensify anisotropy. Anisotropy is usually associated with weak planes also leading to a higher deformability.

The consideration of rock mass anisotropy in rock mass characterization and design of excavation and support is crucial. The neglect can result in a significant underestimation of tunnel wall displacements (2). Although the strong influence of anisotropy has been pointed out by several authors (3, 4, 5), guidelines for the design of excavations in anisotropic rock masses are still missing.

In this paper a short review on methods for modelling anisotropic rock mass is presented. The focus is set on numerical methods, and continuum and discontinuum models are discussed. Anisotropy planes and underground structures can have any relative orientation which calls for three-dimensional models. However, phenomena are discussed on two-dimensional models. These models are representative for situations where the strike of the anisotropy planes is parallel or nearly parallel to the tunnel axis. Due to the higher kinematical freedom of this situation compared to a more general relative orientation, the consequences of anisotropy are more expressed. It should be noted that in two-dimensional simulations the development of displacements with increasing distance from the tunnel face is not covered.

The results of numerical simulations of both continuum and discontinuum models are presented focusing on the influence of discontinuity dip and spacing on the displacement characteristics.

Aspekte zur numerischen Modellierung der Gebirgsanisotropie im Tunnelbau

Für die numerische Modellierung der Gebirgsanisotropie können Kontinuums- und Diskontinuumsmodelle verwendet werden. Welches Modell verwendet werden soll, ist vom Bauwerk und den auftretenden Mechanismen abhängig. Jedes Modell bildet Mechanismen beziehungsweise Verschiebungen auf eine andere Art und Weise ab. Die Unterschiede in der Abbildung werden in einer Parameterstudie genauer beleuchtet. Dabei werden im Speziellen die Verschiebungscharakteristik (Orientierung und Größe), der Versagensmechanismus und die Spannungssituation betrachtet. Anhand dieser Abbildungsunterschiede kann nun je nach Bauwerk ein geeignetes numerisches Modell ausgewählt werden.

The numerical modelling of the anisotropy of rock masses can be simulated with continuum or discontinuum models. These models map the mechanisms with a different scale. Thus, the construction and the corresponding mechanisms shall be considered by the choice of the model. A parametric study with varying dip angle of the discontinuities highlights the capabilities of the models. The capabilities are analysed by distinctions of the displacements characteristic (magnitude and orientation), the failure modes as well as the principal stress tensors. Finally the advantages of the two methods to model anisotropy are summarised. At the end the kind of anisotropy, the project, and the capability of the numerical models shall lead to a suitable choice of the numerical model.

Methods for numerical modelling of rock mass anisotropy

The currently available numerical methods can be classified into methods for continuum models and discontinuum models. The choice of a suitable method for the analysis of excavation in anisotropic rock mass depends on the anisotropy of the rock mass conditions. The applicability of each model has to be judged case by case.

Discontinuum models

In discontinuum models the rock/rock mass and the discontinuities are separately modelled. Consequently, a discontinuum model is a system of blocks which are formed by the intersections of discontinuities. Constitutive laws and material properties are independently assigned to the blocks and discontinuities. Each single block is treated as a continuum which interacts with the others. The coupling between the blocks is controlled by the behaviour of the bounding discontinuities. Typical methods for generating discontinuum models are the distinct element method (DEM) (6) and the discontinuous deformation analysis (DDA) (7).

For the modelling of an anisotropic rock mass one discontinuity set is generated representing the orientation of the anisotropy. In the simulation the rock mass behaviour is controlled by the constitutive laws of the blocks and the discontinuities. The blocks are discretised into finite elements or finite difference zones. The constitutive law of the blocks can be either elastic or elastoplastic. The mechanical behaviour of discontinu-

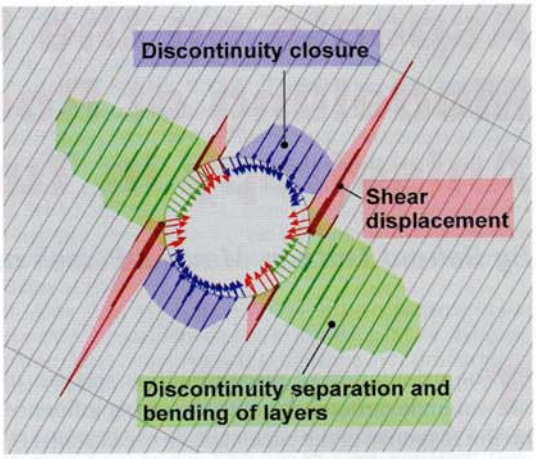

Fig. 1 Stress redistribution in the rock mass results in different kind of mechanisms. The observed displacement vectors at the tunnel wall contain contributions from these mechanisms. In mode 1 (green vectors) discontinuity separation and bending of layers dominates while subordinately the elastic relaxation takes place. In mode 2 (red vectors) the shearing along kinematically free discontinuities and separation has the dominating influence. Elastic relaxation subordinately takes place. In mode 3 (blue vectors) the main contributions result from discontinuity closure and elastic compression.

Bild 1 *Die Spannungsumlagerung im Gebirge verursacht verschiedene Arten von Mechanismen. Die Verschiebungsvektoren an der Laibung beinhalten je nach Ort verschieden große Anteile aus diesen Mechanismen. In Modus 1 (grüne Vektoren) werden die Verschiebungen hauptsächlich durch Trennflächenöffnung und Biegung der Schichten beeinflusst; die elastischen Verschiebungen spielen eine untergeordnete Rolle. In Modus 2 (rote Vektoren) haben Scherverschiebungen entlang kinematisch freien Trennflächen und Trennflächenöffnung den größten Einfluss. Die elastischen Verschiebungen spielen ebenfalls nur eine untergeordnete Rolle. Die Haupteinflüsse in Modus 3 (blaue Vektoren) sind die Trennflächenkompression und die elastischen Verschiebungen.*

ities is described by shear models which include stress-strain relationships perpendicular and parallel to the discontinuity orientation. The simplest relationships are linear elastic springs represented by their stiffness, typically referred to as the discontinuity normal stiffness and shear stiffness. Common nonlinear relationships for the normal stiffness are hyperbolic laws as described by Goodman (8) or Bandis et al. (9).

Continuum models

In continuum models the stress-strain behaviour of the rock mass including the behaviour of the discontinuities are modelled with one constitutive law. The unsteadinesses in stress and displacement field caused by discontinuities are averaged within the material law. Thus, the resulting stress and displacement fields are steady.

Table 1 Material parameters for the blocks and joints.
Tabelle 1 *Materialparameter für das Gestein und die Trennflächen.*

Block Parameters			Joint Parameters		
K	16000	MPa	jkn	5000	MPa/m
G	8000	MPa	jks	2500	MPa/m
c	20	MPa	c	0	MPa
φ	40	°	φ	15	°
σ_t	5	MPa	σ_t	0	MPa

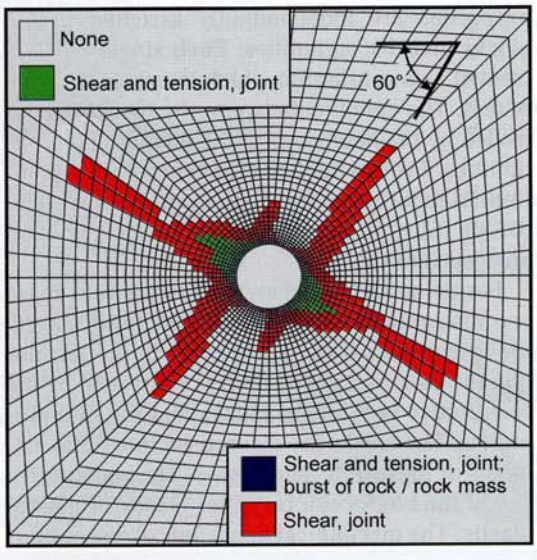

Fig. 2 The dominating failure states distinguished in shear and tension failure of the joints and burst of the rock/rock mass, respectively. In the simulation the effects of the deformed geometry are neglected (small strain).

Bild 2 *Die dominierenden Versagensmechanismen getrennt nach Scher- und Zugversagen in den Trennflächen beziehungsweise Versagen im Gestein. In dieser Berechnung werden die Einflüsse der verformten Geometrie vernachlässigt.*

The effects of the discontinuities and the averaging can affect the elastic and/or the plastic behaviour of the rock mass.

In continuum models the anisotropy is modelled by application of a direction-dependent constitutive law. The elastic anisotropic constitutive laws demand direction-depended properties for Young´s modulus and Poisson´s rate. The plastic anisotropy is modelled by adding a direction-dependent weakness to the constitutive law (e.g. ubiquituous joint law). The direct modelling of spacing with this law is not possible as the name suggests.

Numerical simulations

The Universal Distinct Element Code UDEC (10) is used for simulations of discontinuum models. For the blocks a linear elastic-perfectly plastic constitutive law (Mohr-Coulomb strength criterion with tension cut-off) is applied. The behaviour of the discontinuities is controlled by a spring-slider model where the springs obey a linear elastic relationship. A tension cut-off is applied perpendicularly to the discontinuities while the stress parallel to the discontinuity is limited by the Mohr-Coulomb strength criterion. The basic input parameters for the model are summarized in Table 1. The overburden was chosen to be 600 m which results in a primary vertical stress of 15.9 MPa. The primary horizontal stress is 70 % of the vertical stress (11.1 MPa). The tunnel diameter is 10 m.

The Fast Lagrangian Analysis for Continua in three Dimensions FLAC3D (11) is used for the simulations of continuum models. The constitutive law applied for the rock mass is the same as for the blocks in the discontinuum model. The rock mass properties are also equal to the properties in the discontinuum model (Table 1). The joints are considered with the ubiquituous joint law. The boundary conditions of the model like tunnel diameter, and overburden are the same as used for the discontinuum simulation. A series of simulations was made with different discontinuity dip angles. The influence of the discontinuity spacing on the displacement characteristics was only studied with the discontinuum model.

Failure states and discontinuity displacements

The failure states of the continuum model are compared to the normal and shear displacements of the joints in the discontinuum model.

In the discontinuum model the displacement vectors result from combinations of different discontinuity displacements modes. Figure 1 shows displacements normal to the discontinuity due to discontinuity closure (blue) or separation (green), and shearing parallel to the discontinuity (red). The homogeneous response of the blocks has a minor influence.

The discontinuity displacements mentioned above interact and cause different displacement vector orientations at the tunnel wall. These vector orientations are classified into three modes:

- Mode 1 (green vectors): vectors governed by discontinuity separation,
- Mode 2 (red vectors): vectors governed by shearing on discontinuities and discontinuity separation,
- Mode 3 (blue vectors): vectors governed by discontinuity closure and homogeneous response.

The transition between mode 2 and 3 is rather gradual while the transition between mode 1 and 2 is characterized by an unsteady change of the displacement vector orientation.

The discontinuity separation is a result of stress release and causes also bending of the layers. The bending of two adjacent layers results in shear displacements on the discontinuities reaching deeply into the rock mass.

The failure states of the continuum simulation are presented in Figure 2 for the small strain and in Figure 3 for the large strain calculation mode. These figures show three different failure states; shear failure along the discontinuities in red; shear and tension failure on discontinuities in green, and failure of the rock mass in the blue.

In contrast to the small strain calculation mode failure of the rock mass occurs in the large strain calculation mode (blue zones). This failure leads to additional shear zones at the vertex of the rock mass failure zone.

In the discontinuum and continuum models the failure states and the corresponding displacements occur in comparable regions. The regions of failures are more extended in the continuum simulation due to the ubiquitous material law. The tension failure of the rock/rock mass occurs only as result of buckling. The buckling leads to additional shearing in further distance to the tunnel and thus the shearing areas are increased.

Influence of the discontinuity dip angle

The discontinuity dip was varied from 0 to 90° in 10° increments. The discontinuity spacing was kept at 100 cm for the discontinuum model. In the continuum model the effect of the spacing was assessed by a low cohesion (55 kPa) and tensile strength (18 kPa) of the weak planes. In order to quantify the influence of the dip angles the orientations of the displacement vectors have been evaluated at the crown and both sidewalls.

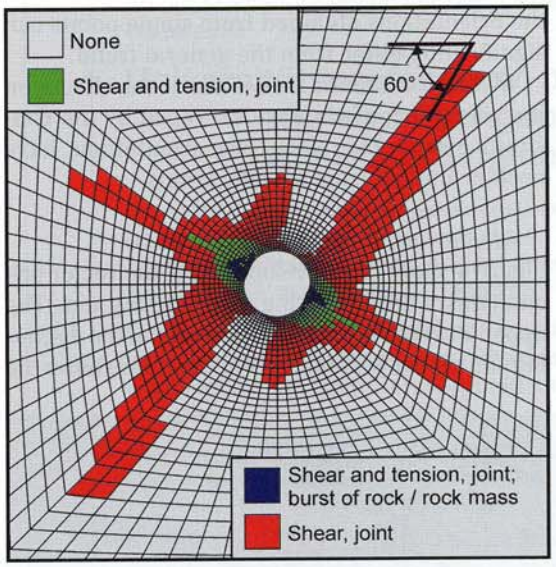

Fig. 3 The dominating failure states distinguished in shear and tension failure of the joints and burst of the rock/rock mass, respectively. In the simulation the effects of the deformed geometry are considered (large strain).

Bild 3 *Die dominierenden Versagensmechanismen getrennt nach Scher- und Zugversagen in den Trennflächen beziehungsweise Versagen im Gestein. In dieser Berechnung werden die Einflüsse der verformten Geometrie berücksichtigt.*

For the discontinuum model the vector orientations have been evaluated from a limited area adjacent to the crown or sidewalls. The representative orientation is defined as the median value of the data set. The spread of the orientations is shown in terms of its standard deviation. The reason for this statistical treatment is that

the orientations obtained from single points can significantly differ from the general trend.

In the continuum model the local effects on the vector orientation are averaged by the constitutive law. Therefore, the orientations have been evaluated from specific points.

Displacement vector orientations

Figure 4 shows the development of the vector orientations with increasing discontinuity dip. The upper diagram represents the result of the discontinuum model while the lower diagram shows the results of the continuum model. For both models with a discontinuity dip of 0° (horizontal discontinuities) the orientation of the displacement vector at the crown is vertical and at the sidewall almost horizontal showing only slight settlements.

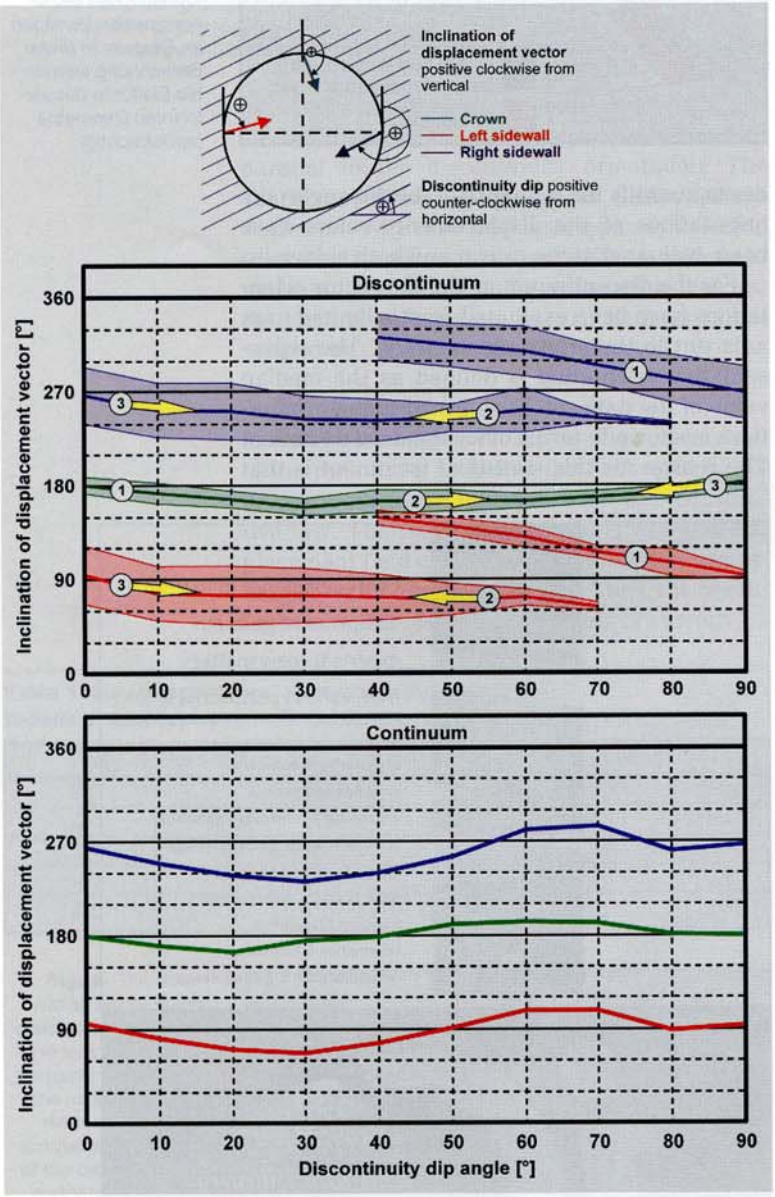

Fig. 4 Development of displacement vector orientation with varying discontinuity dip angle of the discontinuum (upper diagram) and continuum (lower diagram) simulation. The vector orientations are evaluated for the crown and both sidewalls. For the discontinuum simulations additionally a statistically evaluation of the values in the vicinity of the measurement points is performed. Numbers indicate the modes while the arrows indicate the transition between the modes defined in Figure 1.

Bild 4 *Änderung der Orientierung der Verschiebungsvektoren mit unterschiedlicher Trennflächenneigung für Diskontinuums- (oberes Diagramm) und Kontinuumssimulationen (unteres Diagramm). Die Vektororientierung wurde an der Firste und den Ulmen ausgewertet. Zusätzlich wurde für die Diskontinuumssimulation eine statistische Auswertung der Daten in der unmittelbaren Umgebung der Messpunkte durchgeführt. Die Nummern bezeichnen die Modi von Bild 1 und die Pfeile allmähliche Übergänge zwischen den einzelnen Modi.*

In the discontinuum model the influence of the discontinuity separation at the crown (mode 1) is supplemented by shearing (mode 2) from about 20° dip on. With increasing dip the effect of discontinuity separation disappears and gradually the effects of mode 3 become evident. The maximum deviation from vertical is about 20° at 30° dip for the median value. The standard deviation of the orientations is in the range of 8 to 12°. In the continuum model the maximum deviation is also 20° at 20° dip angle. With further increase of the dip angle the vector orientation tends back to the vertical and finally to the left side. The maximum deviation from the vertical to the left occurs at 60° dip angle. The orientation of the crown tends back to vertical when the dip angle approaches 90°.

At the sidewalls of the discontinuum model the influence of discontinuity closure gradually decreases with increasing discontinuity dip and shearing and discontinuity separation becomes more pronounced. The arrows indicate this transition from mode 3 to mode 2. The maximum deviation from horizontal at the right sidewall is about 30° and at the left sidewall 20° (median) while the standard deviation of the orientations is about 20° at maximum. With a dip angle greater than 40° the influence of discontinuity separation without shearing (mode 1) becomes obvious near the sidewalls and is represented by a second branch and labelled with mode 1. These effects are more pronounced with further increasing dip. The deviation from horizontal is about 50 to 60° at 40° dip and almost linearly decreases to horizontal with increasing dip angle. Note that the co-existence of two branches signifies two prominent displacement vector orientations near the sidewalls and represent their unsteady development in discontinuous systems.

In the continuum model the maximum deviation of the vector orientation of the left and the right sidewalls is about 30°. The shape of the orientation looks similar to the orientation of the crown. For a dip angle between 0 to 50° the displacements at the left sidewall tend upwards while those at right sidewall tend downwards. For higher dip angles the trend is vice versa.

The comparison of both models shows a good agreement for the vector orientations from 0 to 40° dip angle. For dip angles from 40 to 90° the displacement vector orientations show an increasing difference. This is explained by the discrete shear displacements in the discontinuum model. For flatter discontinuities mode 1 and mode 3 displacements take place at the crown and sidewalls, respectively. These displacements have only subordinate influence from shearing. For steeper discontinuities mode 2 displace-

ments occur at the sidewalls (indicated by two branches in Figure 4). In the continuum model the effect of these phenomena is averaged resulting in a significant deviation from the orientation obtained from the discontinuum model.

For dip angles steeper than 40° shearing along discontinuities due to kinematical freedom arises. This shearing causes discrete displacements near the sidewall and results in different vector orientation above and below the discontinuity.

Displacement magnitudes

The magnitudes of the crown and sidewalls are taken from single locations of the discontinuum model without any statistical treatment. The evaluation of the magnitude for the continuum models was not performed because the magnitude of the displacements depends on the calculation mode.

In small strain mode the effects of the deformed geometry is neglected. Therefore, buckling is not considered. The large strain mode considers the effects of the deformed geometry. Thus, buckling as fundamental failure mode can occur. It occurs where the discontinuities are tangent to the tunnel, and increases the displacements from about 3 cm in small strain to more than 35 cm in large strain calculation mode.

Mode 1 and 2 mechanisms govern the displacements at the crown for flat discontinuities. The magnitudes gradually decrease from about 4.6 cm to 3.2 cm at 40° dip. Between 40° and 50° dip an unsteady change of the development of the magnitudes is caused by the transition from mode 1 to mode 2. The displacement at 90° dip is about 1.6 cm (Figure 5).

At the sidewalls the magnitudes of the displacements are about 0.65 cm for dip angles lower than 20°. For dip angles from 20 to 60° the magnitudes gradually increase to about 3 cm. Between 60 and 70° dip the transition from mode 2 to mode 1 results in a drop of the displacement magnitudes to about 2.3 cm (see Figure 5).

Principal stresses

Figure 6 displays the principal stress tensors of the discontinuum model. Three regions are identified by distinctive features of the stress tensors. The stress tensors rotated due to shearing along the discontinuities are highlighted in the orange.

The separation of the discontinuities reduces the minimum principal stress and rotates the tensor to be parallel to the discontinuities. These tensors are highlighted in cyan.

As result of the shearing (orange) the stress tensors (green area) are rotated and have a maximum deviation from the discontinuity normal of the discontinuity friction angle.

Figure 7 shows the principle stress tensors of the continuum simulation. The same regions as described above can be identified. In the continuum model the joint-dependent stress tensor rotation (orange) is more gradual because no distinct shear plane can develop (ubiquituous

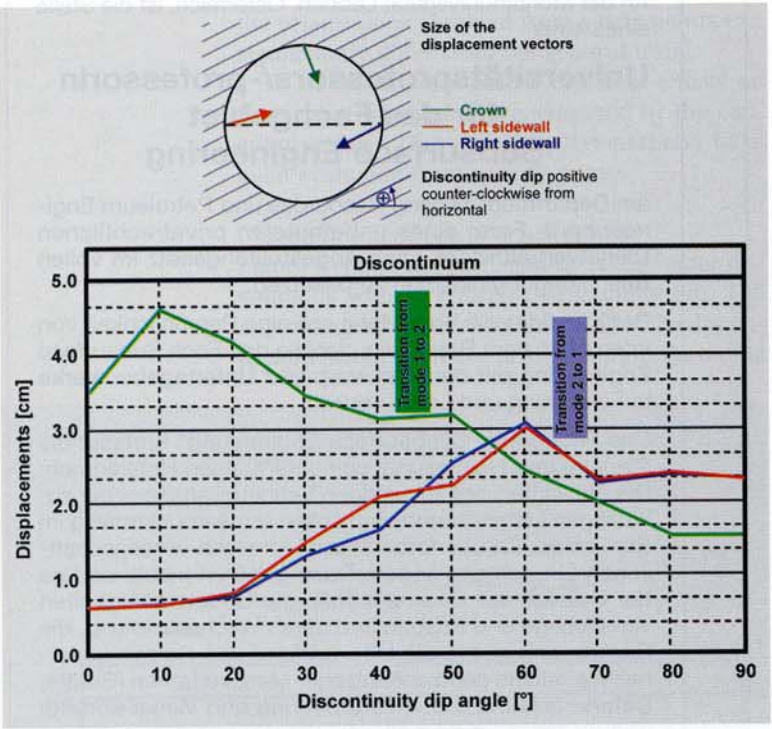

Fig. 5 Development of displacements with varying discontinuity dip angle for the crown and the sidewalls.

Bild 5 *Änderung der Verschiebungsgrößen der Friste und der Ulmen mit unterschiedlicher Trennflächenneigung.*

joints). The tensor rotation due to tensile failure on the discontinuities (cyan) develops further into the rock mass.

Influence of the discontinuity spacing

The discontinuity spacing significantly influences the anisotropic compliance of the rock mass. From a simple elastic point of view the deformability normal to the anisotropy planes in terms of an equivalent modulus of elasticity follows equation 1.

$$E_{\perp} = E \times \frac{s \times k_{nn}}{E + s \times k_{nn}} \quad \text{.....[1]}$$

E is the modulus of elasticity of the host material, s is the discontinuity spacing, and k_{nn} is the linear discontinuity normal stiffness. Using this expression the elastic anisotropic displacements can be determined. However, contributions from discontinuity separation, bending of layers and buckling are not included in this formulation. On the one hand, the limited stress transfer through the discontinuities causes increased stresses parallel to the layers. On the other hand, the thinner layers have a higher slenderness. In addition to bending loads on the layers buckling failure can occur.

Figure 8 shows the dependence of the displacement magnitudes on the discontinuity spacing for a model with a dip angle of 60°. The material properties are equal to those in the previous simulations. Models with spacings of 100, 50, 40, 30, 20 and 10 cm were analysed. The displacement magnitudes are shown for the crown (green) and the sidewalls (blue and red). Additionally, the maximum (orange) and minimum (violet) displacements in the excavation are shown. The black dashed line represents elastic anisotropic displacements perpendicular (using equation [1]) to the discontinuities.

The orange area highlights the difference of the maximum displacements between elastically determined displacements and the results from the numerical simulation. Down to a spacing of

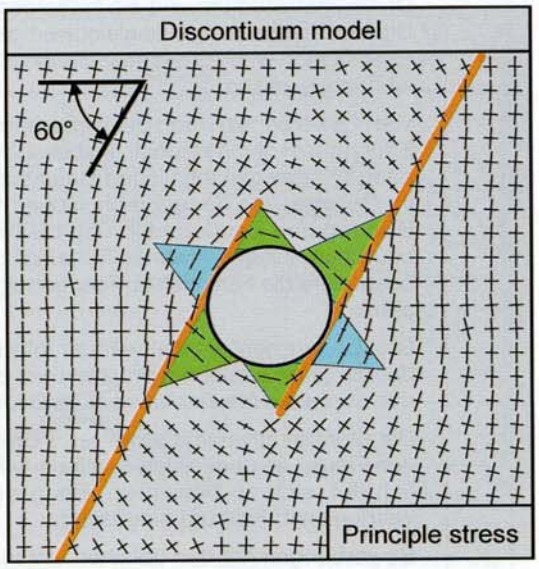

Fig. 6 Principal stress tensors of the discontinuum model with a discontinuity dip angle of 60°. Three areas are identified by distinctive features of the stress tensors: shearing along the discontinuities (orange), discontinuity opening (cyan), shearing and displacements in direction to the tunnel wall (green).

Bild 6 *Hauptnormalspannungen des Diskontinuumsmodells für eine Trennflächenneigung von 60°. Drei Bereiche wurden anhand von Auffälligkeiten der Spannungstensoren unterschieden: Scherung entlang Trennflächen (Orange), Zugversagen der Trennflächen (Cyan), Scherung mit Verschiebungen zum Tunnel (Grün).*

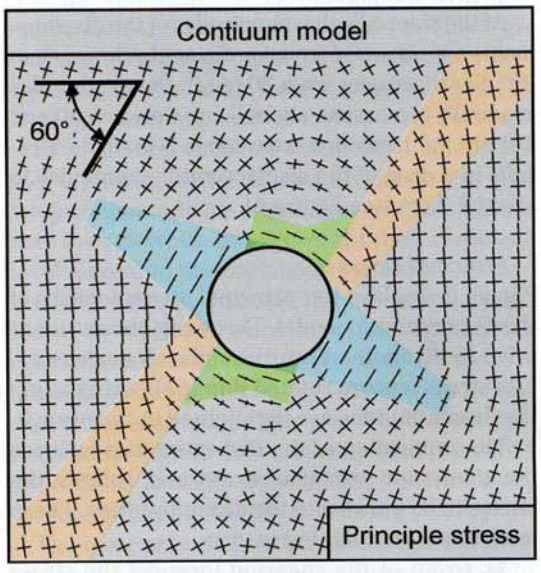

Fig. 7 Principal stress tensors of the continuum model with a discontinuity dip angle of 60°. Three areas are identified by distinctive features of the stress tensors: shearing along the discontinuities (orange), discontinuity opening (cyan), shearing and displacements in direction to the tunnel (green).

Bild 7 *Hauptnormalspannungen des Kontinuumsmodells für eine Trennflächenneigung von 60°. Drei Bereiche wurden anhand von Auffälligkeiten der Spannungstensoren unterschieden: Scherung entlang Trennflächen (Orange), Zugversagen der Trennflächen (Cyan), Scherung mit Verschiebungen zum Tunnel (Grün).*

20 cm the difference gradually increases. With decreasing spacing the influence of shearing along kinematically free discontinuities on the radial displacements decreases. The influence of bending or buckling of the layers on the radial displacements increases.

Buckling leads to stress concentrations further apart from the excavation boundary. At this point a change of failure mechanism takes place including the development of secondary shear planes.

The displacement magnitudes in the discontinuum model can be split into portions originating from different mechanisms. Shear displacements take only place at kinematically free locations. Displacements from bending or buckling are influenced by discontinuity spacing. The governing mechanism on the displacements can be clearly addressed. In contrast, the continuum model with the ubiquituous joint approach judges the governing displacement at the elements assuming omnipresent weakness planes. Displacements in the plastic regions are only dominated by the plastic flow and do not take into account the mechanisms occurring in the rock mass. Although it is supposed that displacement magnitudes can be controlled by the parameters of the ubiquituous joint, a clear correlation between those parameters and the discontinuity spacing could not be found.

Conclusion

In the preceding chapters results from numerical simulations with continuum and discontinuum models have been presented.

Coincidences are only found for specific dip angles and single results such as the displacement vector orientations at the crown for a dip angle of 40°. The differences in the results arise from the capabilities of each model to represent the rock mass behaviour. Especially, the different consideration of the flexural stiffness of the rock mass layers and the discrete displacements along the discontinuities cause deviations.

To decide the suitable method for the specific simulation, the dominating mechanism has to be identified:

- If the mechanism strongly depends on the spacing (flexural stiffness or discrete displacements), the discontinuum model should be preferred.
- The continuum model should be chosen, when the strength of the rock mass is determined by small scale buckling on various locations e.g. thinly layered schist or phyllites.

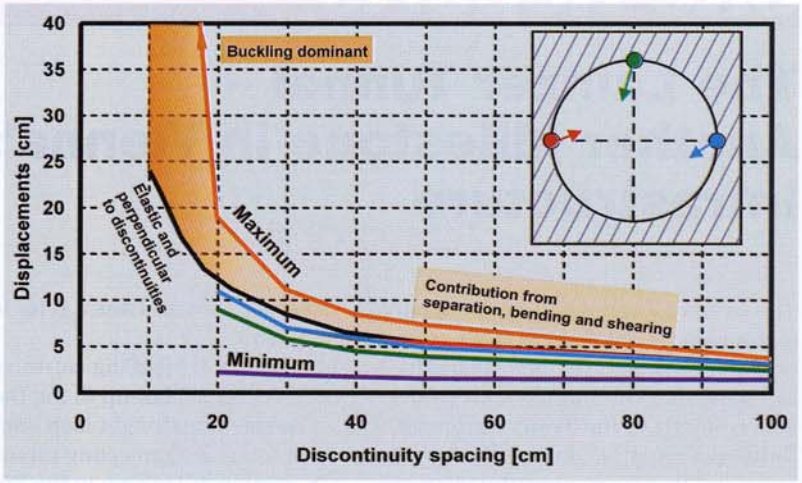

Fig. 8 Development of the displacement magnitudes with varying discontinuity spacing for a dip angle of 60°.

Bild 8 *Änderung der Verschiebungsgrößen mit unterschiedlichem Trennflächenabstand bei einer Trennflächenneigung von 60°.*

References

1. Goricki, A. ; Button, E.A. ; Schubert, W. ; Pötsch, M. ; Leitner, R.: *The Influence of Discontinuity Orientation on the Behaviour of Tunnels*. Felsbau 23 (2005), No. 5, pp. 12-18.
2. Huber, G. ; Westermayr, H. ; Alber, O.: *Einfluss der Gefügeorientierung am Strenger Tunnel*. Felsbau 23 (2005), No. 5, pp. 20-24.
3. Button, E. ; Blümel, M.: *Characterization of phyllitic and schistose rock masses: from system behaviour to key parameters*. Schubert (ed.): Proc. EUROCK 2004 & 53rd Geomechanics Colloquium, October 7-9, 2004, Salzburg, Austria, pp. 459-464. Essen: Verlag Glückauf GmbH, 2004.
4. Everitt, R.A. ; Lajtai, E.Z.: *The influence of rock fabric on excavation damage in the Lac du Bonnett granite*. Int. J. Rock Mech. Min. Sci. 41 (2004), No. 8, pp. 1277-1303.
5. Tonon, F. ; Amadei, B.: *Stresses in anisotropic rock masses: an engineering perspective building on geological knowledge*. Int. J. Rock Mech. Min. Sci. 40 (7-8), 2003, pp. 1099-1120.
6. Hart, R.D.: *An Introduction to Distinct Element Modelling for Rock Engineering*. Hudson, Brown, Fairhurst & Hoek (eds.): Comprehensive Rock Engineering, Volume 2 , 1993, pp. 245-261.
7. Shi, G.-H.: *Block System Modelling by Discontinuous Deformation Analysis*. Computational Mechanics Publications. London, 1993.
8. Goodman, R.E.: *Methods of geological engineering in discontinuous rocks*. St. Paul: West Publishing Co.
9. Bandis, S.C. ; Barton, N.R. ; Christianson, M.: *Application of a new numerical model of joint behaviour to rock mechanics problems*. Stephansson (ed.): Proc. Int. Symp. on Fundamentals of Rock Joints, September 15-20, 1985, Björkliden, Sweden, pp. 345-355.
10. Itasca Consulting Group, Inc.: *Universal Distinct Element Code (UDEC)*. Version 4.0. Minneapolis, Minnesota, 2004.
11. Itasca Consulting Group, Inc.: *Fast Lagrangian Analysis for Continua in three Dimensions (FLAC3D)*. Version 2.1. Minneapolis, Minnesota, 2002.

Authors

Dipl.-Ing. Roland Leitner, Dipl.-Ing. Markus Pötsch, o.Univ.-Prof. Dipl.-Ing. Dr.mont. Wulf Schubert, Institute for Rock Mechanics and Tunnelling, Graz University of Technology, Rechbauerstraße 12, A-8010 Graz, Austria, E-Mail r.leitner @tugraz.at; m.poetsch@tugraz.at; schubert@tugraz.at